ELSEVIER

Journal of Hazardous Materials B103 (2003) 43–63

Journal of Hazardous Materials

www.elsevier.com/locate/jhazmat

Multi-functional sorbents for the simultaneous removal of sulfur and lead compounds from hot flue gases

Yi Zhao*, Wen-Chiang Lin

Department of Chemical Engineering, Wu-Feng Institute of Technology, 117 Chian-Kuo Road, Sector 2, Min-Hsiung, Chiayi 621, Taiwan, ROC

Received 22 October 2001; received in revised form 10 December 2002; accepted 16 December 2002

Abstract

A multi-functional sorbent is developed for the simultaneous removal of $PbCl_2$ vapor and sulfur dioxide from the combustion gases. The sorbent is tested in a bench-scale reactor at the temperature of 700 °C, using simulated flue gas (SFG) containing controlled amounts of $PbCl_2$ and SO_2 compounds. The removal characteristics of $PbCl_2$ and SO_2, individually and in combination, are investigated. The results show that the mechanism of capture by the sorbent is not a simple physical adsorption process but seems to involve a chemical reaction between the Ca-based sorbent and the contaminants from the simulated flue gas. The porous product layer in the case of individual SO_2 sorption is in a molten state at the reaction temperature. In contrast, the combined sorption of lead and sulfur compounds generates a flower-shaped polycrystalline product layer.

Keywords: Adsorption; Sulfur; Lead; Lime; Sorbent

1. Introduction

Lead compounds are considered to be among the most toxic trace elements introduced into the atmosphere from incineration and other industrial discharges. Lead salts of long chain organic acids are used as stabilizers in the plastic industry. Large quantities of lead compounds are also consumed in the manufacture of storage batteries and pigments [1]. When wastes containing lead compounds are incinerated, various lead compounds are formed. The chemical form and concentration of these compounds depend mostly on waste composition and operating conditions [2]. Chemical equilibrium analysis shows that when

* Corresponding author. Fax: +886-5-2264224.
E-mail address: c9418@ms41.hinet.net (Y. Zhao).

0304-3894/$ – see front matter © 2003 Published by Elsevier B.V.
doi:10.1016/S0304-3894(03)00088-8

chlorine-containing wastes are incinerated, lead compounds exist predominantly as PbO, $PbCl_2$ and $PbCl_4$ in the flue gases [3]. A promising and unique technique for metal vapors removal from high-temperature flue gases is to use solid sorbents to capture metal compounds through a combination of adsorption and chemical reactions [4].

There have been studies on the reaction of lead compounds with different sorbents. Holland et al. [5] studied the chemical reaction of lead oxide with kaolinite, an aluminosilicate clay, by heating the powders of these compounds to high temperatures. Their results indicate that PbO reacts readily with kaolinite at 650 °C, forming the compounds $4PbO{\cdot}Al_2O_3{\cdot}2SiO_2$ and $PbO{\cdot}Al_2O_3{\cdot}2SiO_2$. With additional Al_2O_3, a new compound $PbO{\cdot}Al_2O_3{\cdot}SiO_2$ is formed. Cantwell and Jacobs [6] demonstrated that alumina pellets can be used as lead traps for control of particulate lead emissions from automobile exhausts.

Uberoi and Shadman [4,7] investigated the potential of several simple sorbents (silica, alumina, kaolinite, bauxite emathlite, and limestone) for lead capture and found that, except limestone, all are effective for lead removal from hot flue gases. Scotto and Uberoi [8] also conducted a series of experiments using a bench-scale thermogravimetric reactor and a pilot-scale combustor. In their bench-scale study, both kaolinite and bauxite were found to be effective for lead chloride removal at 800 °C. They also showed that the combined usage of silica and alumina greatly enhances the overall capacity.

Linak [9] studied the capture of nickel, cadmium, and lead using various sorbents in a laboratory swirl flame incinerator. Kaolinite was demonstrated to be effective but the presence of chlorine was found to inhibit and reduce the effectiveness of capture. Ho et al. [10] demonstrated the capture of lead species in a fluidized bed of sorbent materials. They concluded that the calcinated limestone is better than alumina and sand in capturing lead species. Maximum capture occurred at an optimal temperature range of 600–800 °C.

Research in recent years has been focused toward finding multi-functional sorbents suitable for simultaneous removal of several air toxins. Because calcium-based sorbents have been extensively applied in removal of acidic gases from flue gases, they offer a practical alternative for use as multi-functional sorbents due to their effective performance in capturing sulfur and lead species. The results by Agnihotri et al. [11] showed that, in sorption of selenium oxide by Ca-based sorbents in the presence of SO_2, formation of $CaSeO_3$ is considerably slower than the sulfation of the sorbent when the concentration of the two species (SeO_2 and SO_2) in the gas phase is comparable. Wu and Shadman [12] extended their earlier studies to the development of a multi-functional sorbent for capture of sulfur dioxide, alkali metals and lead. This aluminosilicate sorbent was effective in simultaneous removal of the species, and no loss of activity was observed due to competitive reactions.

Sulfation kinetics of calcium-based sorbents has been extensively investigated, but studies regarding the interactions of lead compounds with these sorbents under typical flue gas environment are still lacking. In the actual flue gas atmosphere, Ca-based sorbents can react with a host of constituents, and the extent to which one particular species is captured depends greatly on the kinetics of the reaction between the species and the sorbents. It is very well documented that the sulfation reaction of Ca-based sorbents is rapid [13,14]. To realize the role of Ca-based sorbents in multi-functional sorption and to determine the effectiveness of these sorbents in removing lead species from the flue gases, it is imperative that interactions among lead, sulfur compounds and these sorbents be fully studied. Furthermore, the

investigation must be carried out for the simultaneous removal of SO_2 and lead compounds from hot flue gases to realize the potential multi-functional role of Ca-based sorbents.

In the first part of this study, a number of sorbents were screened and compared for their effectiveness in removing lead compounds from hot flue gases. Because of the high effectiveness of CaO in lead capture, details of the reaction mechanism between CaO and $PbCl_2$ at temperature of 700 °C were also investigated.

The second part of this study was to develop a multi-functional sorbent for removal of sulfur and metallic contaminants and to examine the removal characteristics of lead and sulfur dioxide, first separately and individually and then in combination and simultaneously.

2. Experimental approach

2.1. Apparatus

A schematic diagram of the experimental setup is shown in Fig. 1 [4]. It has three sections. The first is for preparing a simulated flue gas (SFG) with a controlled flow rate

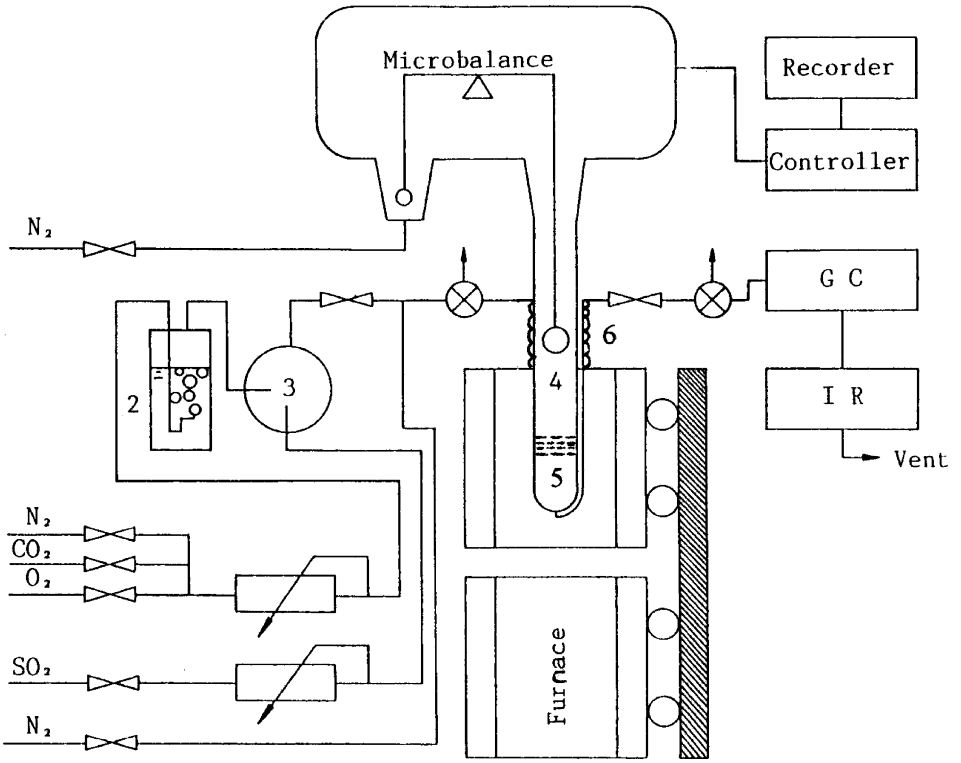

Fig. 1. Schematic diagram of the experimental apparatus: (1) mass flow controller; (2) saturator; (3) mixer; (4) the source of vaporized $PbCl_2$; (5) sorbent bed; (6) temperature controller.

and composition. This section consists of the mass flow controllers, a moisture introduction cell, a gas mixer and a Perkin-Elmer AD6 digital microbalance. The SFG enters the reactor from the left inlet and mixes with the vaporized $PbCl_2$ from a suspended platinum pan. The pan is suspended by a Pt hangdown wire from the digital microbalance. $PbCl_2$ is used as the lead source in all the experiments. The upper part of the reactor containing the lead source is wrapped with heating tape and maintained at a specific temperature using a thermal couple and a temperature controller. The desired concentration of $PbCl_2$ in the gas phase dictates the temperature at which the vaporization of $PbCl_2$ is maintained. The chamber containing the source metal has been designed and tested to make sure that vapor delivery rate to the inlet gas remains constant during the course of an experiment. An auxiliary vent connected to the exhaust is included in the reactor system. This allows the lead-laden flue gas to pass through the sorbent bed only when a steady source evaporation rate has been achieved.

The second section is a reactor system. The quartz reactor is inside a movable electric furnace (LINDERG HIF-55322C) which can be moved up and down for the rapid startup and quenching of the reaction. The reaction bed consists of two thin annuluses. The first annulus made of quartz is welded to the inner surface of the quartz reactor. The second annulus made of stainless steel is placed on top of the first one. The sorbent is dispersed on a 100-mesh stainless steel screen which is welded to the second annulus. The reactor system in this study is a flow-through system [4] as opposed to a flow-over system [12] as is the case in studies carried out in a thermal gravimetry-based reactor system. The gas coming out from the reactor passes through a train of scrubbers to capture the remaining $PbCl_2$ prior to being vented to exhaust.

The third section is for the gas analysis and data acquisition. The gas analysis consists of the gas chromatograph (SHIMADZU, GC-8A) and an infra-red analyzer (JAPAN JASCO IR-700).

Other analytical equipments used include a scanning electron microscope (JEOJ JSM-35 SEM) equipped with energy dispersive X-ray (EDX) and a scanning Auger microprobe (FISON MICROLAB 310D) for the detailed study of the captured metal and sulfur distribution in the sorbent particles.

For scanning electron microscopy analysis, the powdered samples have been coated with platinum and examined with a Philips XL 40 instrument operated at a potential of 15–20 kV. Ultimate resolution should be near 30 nm. A X-ray diffractometer (RIGAKU D/MAXIII VXRD) with a Cu Kα source was also used to identify the principal crystalline phases formed during the sorption process.

2.2. Reactants

2.2.1. Gaseous reactants

The flue gas used in this study consisted of 80% N_2, 15% CO_2, 3% O_2, and 2% H_2O. The flue gas was humidified by blowing it through a vessel containing water prior to entering the reactor system.

2.2.2. Sorbents

In the first part of this study, a number of naturally available materials and model compounds were tested as potential sorbents for removal of lead compounds from hot flue gases.

Table 1
Composition of sorbents (as received from Fluka (Riedel-deHäen) Company)

	Silica (wt.%)	Alumina (wt.%)	CaO (wt.%)	Kaolinite (wt.%)
SiO_2	>99.9	–	–	7.259
Al_2O_3	–	>99.9	–	56.75
CaO	–	–	97.0	–
Fe_2O_3	–	–	–	6.20
TiO_2	–	–	–	0.50
Impurity	–	–	3.0	29.30

The model compounds included silica and alumina. The naturally available sorbents are kaolinite and lime. The composition of these sorbents is given in Table 1. The sorbent particles, 60–80 mesh in size were calcined at 900 °C for 2 h and stored under vacuum until used.

2.2.3. Activated sorbents

In the second part of this study, the additive ($CaCl_2$) was added to CaO by impregnation with a solution of $CaCl_2$. The quantity of the additive was 2 mol%, i.e. 2.2 g $CaCl_2$ (MW = 111) dissolved in a certain amount of water for 56 g CaO (MW = 56).

2.3. Analysis of the products

The amount of lead captured was determined by measuring the lead content of the sorbents after the experiment. The water soluble fraction of the adsorbed lead was determined by leaching with deionized water. The total lead capture was determined by dissolving 20 mg of the sample in a $H_2O/HF/HNO_3$ (2/1/1 proportion by volume) mixture of 50 ml. For water leaching experiments, 20 mg of the sample was placed in a ultrasonic bath in a beaker filled with 100 ml of deionized water at 40 °C for 4 h. A GBC 908 atomic absorption spectrophotometer was used in the absorption mode for the determination of lead content of the sorbents.

Sulfate analyses were performed on the samples by $Ba(ClO_4)_2$ titration on the remaining solution after removal of Ca^{2+} with ion exchange resin. Titrations were carried out according to the standard procedures [15].

Differential scanning calorimetry (LT-Modulate DSC 2920) technique was employed to determine the melting point of a mixture of $CaCl_2$ and $CaSO_4$.

2.4. Experimental procedure

Each experiment was initiated by first starting the carrier gas flow to purge the reactor system. The preheated furnace was then raised to heat the sorbent particles. Heating of the lead source subsequently began to vaporize $PbCl_2$ which was carried through the fixed bed of sorbents by the SFG. After a predetermined amount of the source compound had vaporized, the adsorption experiment was terminated by lowering the furnace and diverting the gas flow through the auxiliary vent. In all experiments, the gas flow rate in the reactor and around the sorbents particles was kept at 190 ml/min.

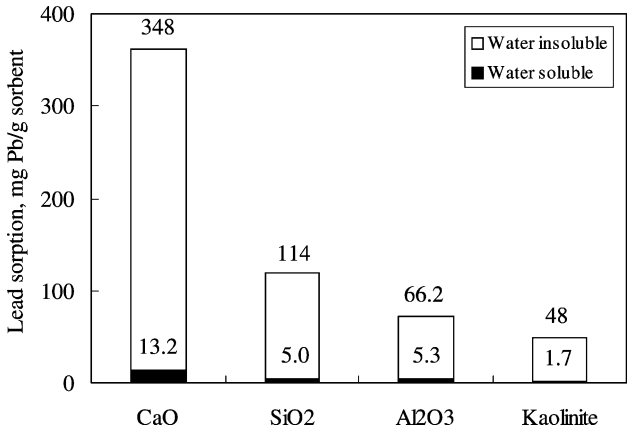

Fig. 2. Lead uptake by various sorbents in 2 h; $T = 700\,^{\circ}C$; concentration of $PbCl_2$: 3.3×10^{-5} g mol/l.

3. Results and discussion

3.1. Screening experiment

The results obtained from the screening experiments are shown in Fig. 2. They indicate good reproducibility from the multiple experiments conducted with most of the sorbents. Since all experimental parameters except the sorbent type were kept constant, the amount of lead adsorbed clearly indicates the sorbent effectiveness for lead removal from hot flue gases. The most distinct feature of the results is the difference in abilities of the sorbents to capture lead from the flue gas passing through them. Of the two model compounds, silica exhibits a higher lead capturing efficiency than alumina. Of the other two naturally available materials, lime has a much higher efficiency for lead capture than kaolinite. Among the four sorbents tested, lime exhibits superior lead sorption capability. Ho et al. [10] also demonstrated that the calcined limestone (CaO) is better than alumina and sand in capturing lead with a fluidized bed incinerator.

The water solubilities of lead compounds adsorbed by these sorbents range from 3.5 (kaolinite), 3.8 (CaO), 4.4 (SiO_2) to 8.0 wt.% (Al_2O_3), respectively. It should be pointed out that the leaching of lead from the spent sorbents might cause the environmental problems. However, the spent sorbents could be solidified first and then be disposed of in a sanitary landfill or monofill.

Based on the overall capacity for lead removal and water solubility of the products, it seems that lime is the most effective for immobilizing the lead species and is therefore chosen for further mechanistic studies which are described later.

To gain insight into the mechanism of reaction of $PbCl_2$ with CaO, the SEM technique was used to obtain information on the morphological change of lime particles after adsorption. Fig. 3 shows a typical SEM image of the surfaces of lime particles prior to lead sorption. After calcination at 900 °C, lime has an irregular surface with numerous cracks. The width of the cracks is in the order of 20 μm. Fig. 4 is a typical SEM image of the surfaces of partially

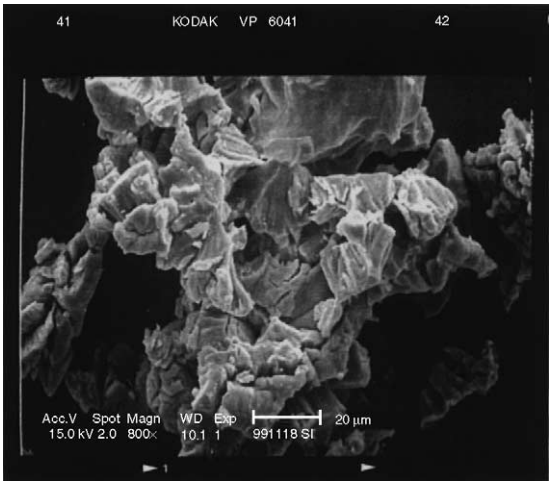

Fig. 3. Scanning electron micrograph of a fresh lime particle. Magnification 800×.

converted lime particles. It reveals that after reaction a porous surface has changed to the rugged morphology, with the formation of the products on the lime surfaces and a complete disappearance of the cracks. As shown by XRD analysis to be discussed later, the main component of the final products is calcium plumbate (Ca_2PbO_4). Since the molar volume of calcium plumbate is higher than that of calcium oxide, the formation of calcium plumbate on the lime surfaces blocks the sorbent pores, resulting in incomplete sorbent utilization. For in situ applications, the efficiency of the sorbents can be increased by decreasing the particle size. Fig. 5 shows a X-ray Kα map of calcium on the surfaces of the lime particles

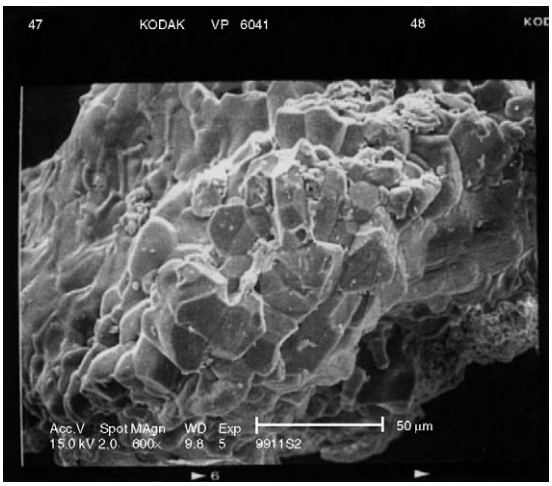

Fig. 4. Scanning electron micrograph of a partially converted lime particle. Magnification 600×.

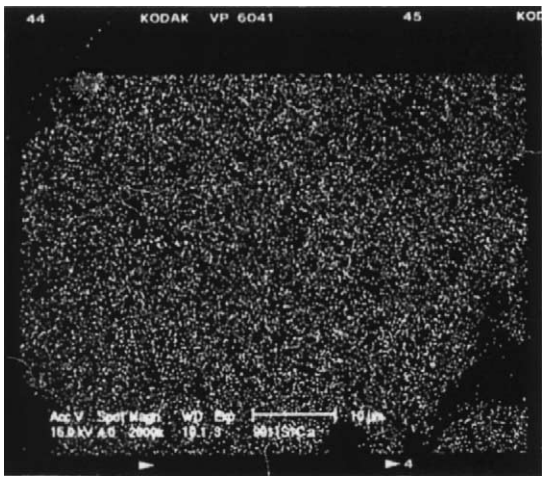

Fig. 5. Ca Kα X-ray map of a fresh lime particle.

prior to lead reaction. Figs. 6 and 7 are X-ray Kα maps of calcium and lead on the surfaces of partially converted lime particles. They confirm the presence of lead on the lime surfaces and reveal a nonuniform distribution of the two elements on the lime surfaces after lead sorption. Comparison of calcium map with lead one shows that the regions high in lead have low concentrations of calcium. A scanning Auger microprobe survey of the particles after lead adsorption also showed a variation of the lead concentration on the lime surfaces.

In order to gain further insights into the actual mechanism of Pb/lime interaction, XRD was used to identify the final products formed by sorption of lead chloride on lime. As

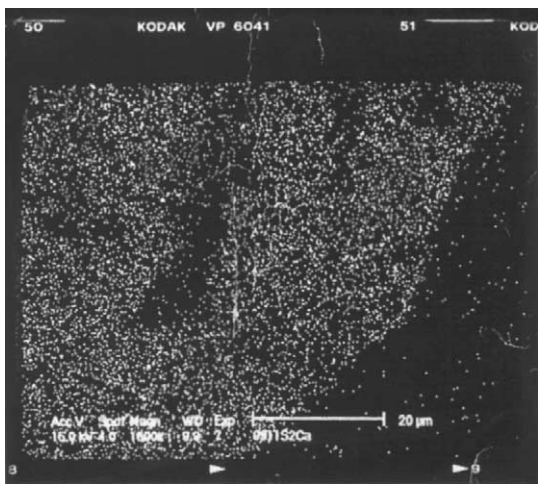

Fig. 6. Ca Kα X-ray map of a partially converted lime particle shown in Fig. 4.

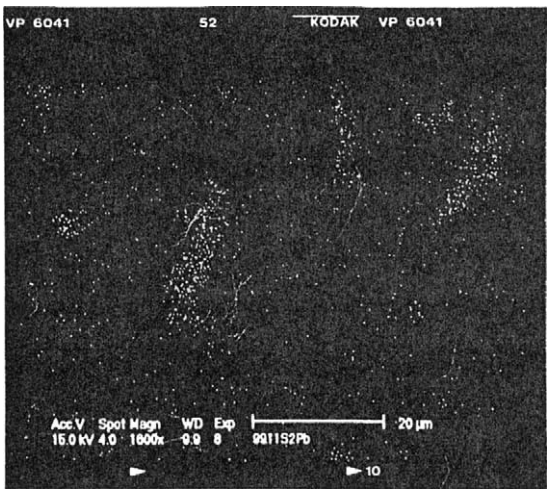

Fig. 7. Pb Kα X-ray map of a partially converted lime particle shown in Fig. 4.

shown in Fig. 8, the XRD diffractogram of the lime particles, which were exposed to lead chloride vapors for 4 h at 700 °C at the lead concentration of 3.3×10^{-5} g mol/l, indicated the formation of calcium plumbate as a major product and Pb_2O_2Cl as a minor one. Incidentally, an Auger microprobe survey of the lime particles exposed to lead vapors did show a small percentage of chlorine signal. This seems to confirm the existence of Pb_2O_2Cl on the converted lime surfaces. Ho et al. [10] pointed out that in a high-temperature environment in the presence of air, lead chloride would react with oxygen to form different kinds of lead oxychlorides and lead oxide. Therefore, it is concluded that the Pb_2O_2Cl observed from XRD analysis was formed in the gas phase and condensed on the lime surfaces. On the other hand, no $PbCl_2$ is observed on the reacted samples, indicating that the physical adsorption or condensation of $PbCl_2$ vapor on the lime surfaces is not a predominant sorption mechanism.

The actual mechanism of lead sorption by CaO could involve either physisorption of $PbCl_2$ or some chemisorbed complex or some chemical reaction products from the reaction between CaO and $PbCl_2$ or a combination of all these phenomena.

The above results show that CaO is a good sorbent for lead compounds capture. However, it is only effective to a certain degree because of the pore plugging caused by formation of Ca_2PbO_4 and Pb_2O_2Cl. Since CaO is a practical sorbent for capture of both $PbCl_2$ and SO_2, it is very natural and pragmatic to modify the nature of the lime particles to alleviate the problems of the pore plugging by use of additives. It is this motivation that leads to the studies in the second part of this paper.

3.2. Adsorption of individual compounds through the multi-functional sorbent

The experiments in this section were designed to determine the effectiveness of the multi-functional sorbents for the removal characteristics of toxic metal (lead) and sulfur dioxide, first separately and individually and then in combination and simultaneously.

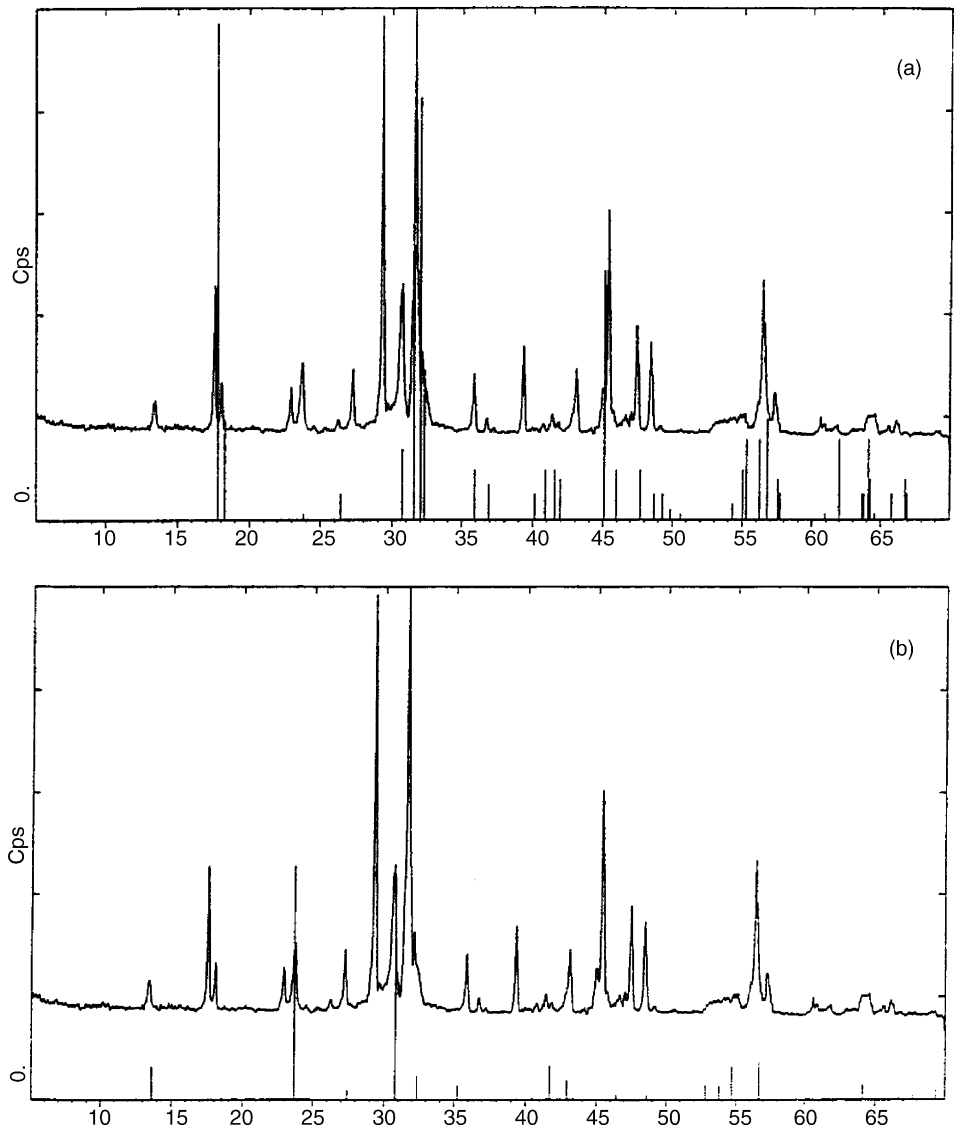

Fig. 8. (a) X-ray diffraction pattern of partially converted lime particles and the standard XRD pattern of Ca_2PbO_4; (b) X-ray diffraction pattern of partially converted lime particles and the standard XRD pattern of Pb_2O_2Cl. Sorption conducted at 700 °C for 2 h at 3.3×10^{-5} g mol/l of $PbCl_2$.

The SO_2 removal efficiency of CaO (pure or doped) is shown in Fig. 9. It shows the influence of $CaCl_2$ on the reactivity of CaO in presence of SO_2 at 700 °C. The acceleration of the rate of fixation of SO_2 on the lime particles is dramatic. The results also indicate that both the initial rate and the adsorption capacity are greatly increased by addition of $CaCl_2$

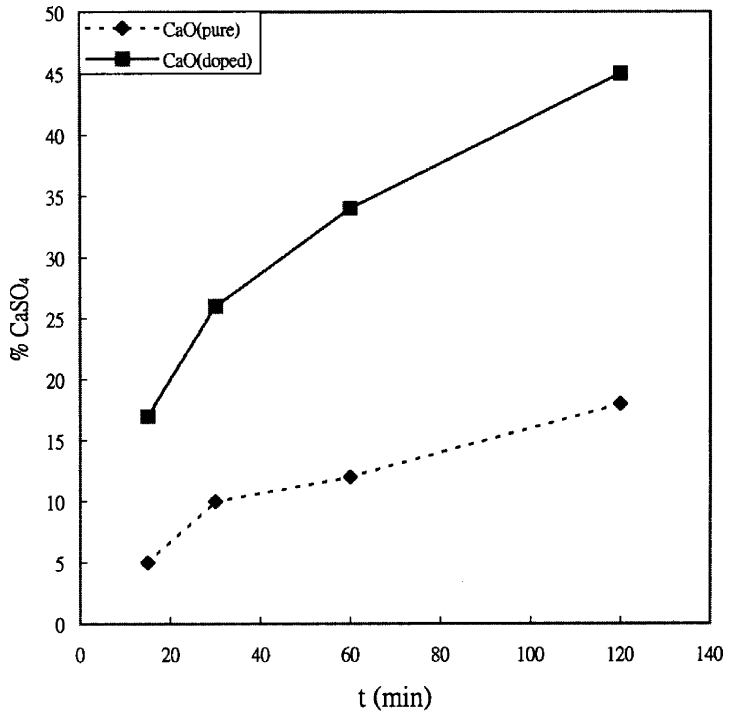

Fig. 9. Reaction of CaO, either pure (dashed line) or impregnated with 2 mol% $CaCl_2$ (solid line), with SO_2.

at 700 °C. The adsorption capacity of the modified CaO is 2–5 times greater than that of the original CaO for the reaction duration of 10–60 min.

In order to gain further insights into the mechanism of SO_2/lime interactions, the XRD technique was used to identify the final products formed during the sulfation. As shown in Fig. 10, the XRD diffractogram of the lime particles, which were exposed to SO_2 at 700 °C for 10 and 20 min, indicates the formation of calcium sulfate and calcium carbonate. The formation of calcium carbonate is through the following reaction:

$$CaO + CO_2 \rightleftarrows CaCO_3 \tag{1}$$

whereas the formation of calcium sulfate is based on the following two reactions [16]:

$$CaO + SO_2 + \tfrac{1}{2}O_2 \rightleftarrows CaSO_4 \tag{2}$$

$$\left.\begin{array}{l} CaCO_3 + SO_2 \rightarrow CaSO_3 + CO_2 \uparrow \\ CaSO_3 \xrightarrow{+0.5O_2} CaSO_4 \\ \text{or} \\ CaSO_3 \xrightarrow{+0.5SO_2} CaSO_4 + 0.5S \downarrow \end{array}\right\} \tag{3}$$

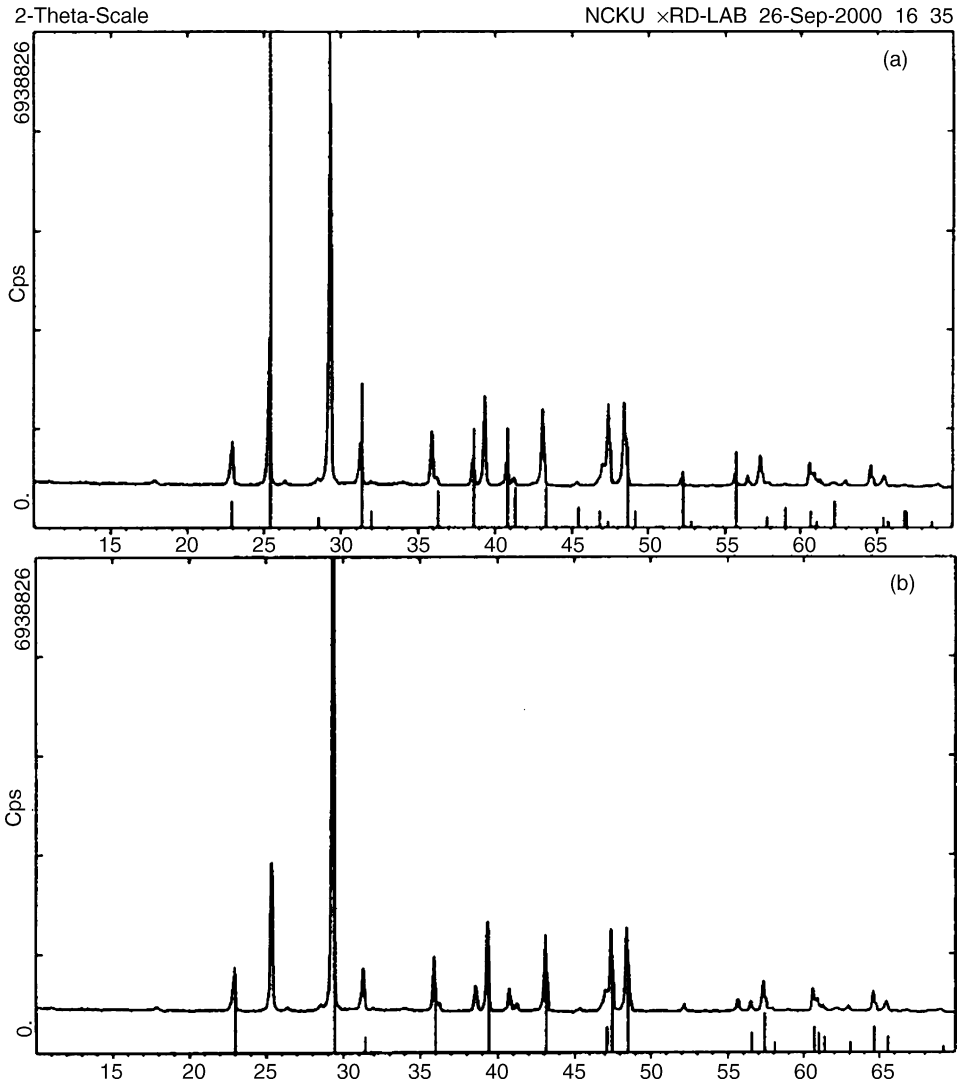

Fig. 10. (a) X-ray diffraction pattern of partially converted lime particles and the standard XRD pattern of $CaSO_4$; (b) X-ray diffraction pattern of partially converted lime particles and the standard XRD pattern of $CaCO_3$.

To get a better understanding of the mechanism of this dramatic acceleration, the SEM technique is used to obtain information on the structural change of doped lime particles during the sulfation.

Fig. 11(a) is a typical SEM image of the surfaces of partially converted lime particles after SO_2 sorption. It shows that morphological features of the surfaces of the lime particles remain similar to those of the original lime particles as shown in Fig. 3. However, the width of the cracks after reaction becomes much smaller. This is due to the fact that the

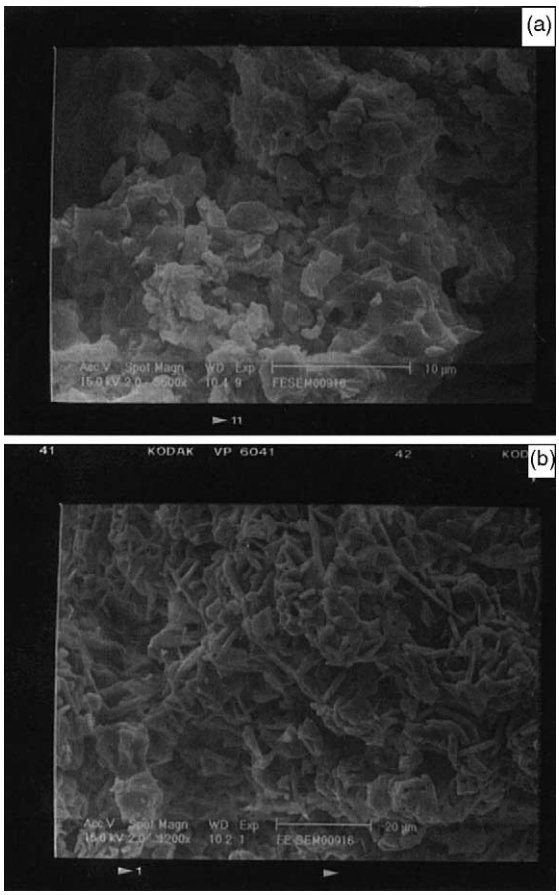

Fig. 11. Morphological change in the surface of CaO. (a) After 20 min of SO_2 adsorption, CaO (pure), $T = 700\,^{\circ}C$, magnification 3500×; (b) after 20 min of SO_2 adsorption, CaO (impregnated with 2 mol% $CaCl_2$), magnification 1200×.

molar volumes of calcium carbonate and calcium sulfate are larger than that of calcium oxide.

Fig. 11(b) is a representative SEM image of the surfaces of partially converted lime particles (doped with $CaCl_2$) after SO_2 sorption. It shows that an original aspect of pure CaO has completely disappeared, resulting in a deep alteration of the surfaces. It can also be observed that the more voids were formed in the course of sulfation of the doped CaO. The product layers seem to be in a molten state at the reaction temperature. This observation is in contrast with what is observed in the sorption of SO_2 on the pure CaO. By means of DSC technique, we also noted that a mixture of $CaCl_2$ and $CaSO_4$ (with the molar concentration of $CaCl_2$ varying from 10 to 50%) melted at 997 K (724 °C), which is much lower than the melting point of $CaCl_2$, 1045 K (772 °C) and that of $CaSO_4$, 1723 K (1450 °C). This proves that $CaCl_2$ forms a eutectic phase with $CaSO_4$ at temperatures much lower than the melting

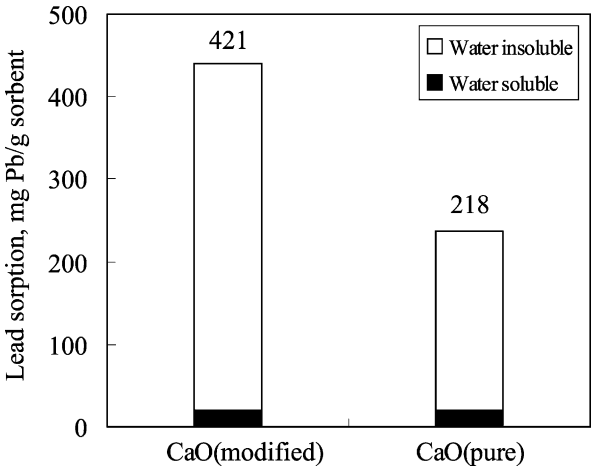

Fig. 12. Lead uptake by CaO (either pure or impregnated with 2 mol% $CaCl_2$) in 40 min, $T = 700\,^{\circ}C$, concentration of $PbCl_2$: 8.1×10^{-5} g mol/l.

point of either $CaCl_2$ or $CaSO_4$. The formation of the molten phase helps the generation of more voids throughout the structure of the lime particles, thus facilitating the diffusion of SO_2 toward the interior of the lime particles.

We have made another attempt for determining whether $CaCl_2$ was able to react with the gas phase (consisting of N_2, SO_2, and O_2). $CaCl_2$, after its exposure to the gases, remained unchanged. It is therefore concluded that there is no interaction between SO_2, O_2 and $CaCl_2$. This is consistent with the results of Derlyukova [17], who did not observe any chemical reaction between SO_x, O_2 and $CaCl_2$ (20–850 °C), unless an oxidation catalyst was added.

Fig. 12 shows the lead uptake by the pure CaO as well as the doped CaO under the flue gases of this study at 700 °C. The doped CaO exhibits much higher capture capacity of lead as compared to the pure CaO. The water solubility of lead adsorbed by these two sorbents is less than 3.5 wt.%.

As shown in Fig. 13, the XRD diffractogram of the lime particles (pure or doped) exposed to $PbCl_2$ at 700 °C indicates that the major phases identified are $CaCO_3$ and Ca_2PbO_4. The mechanism of $CaCO_3$ formation has been discussed earlier. To explain the formation mechanism of Ca_2PbO_4, the following reaction schemes are proposed:

$$2CaO + PbCl_2 + O_2 \rightarrow Ca_2PbO_4 + Cl_2 \quad (4)$$

$$2CaCO_3 + PbCl_2 + O_2 \rightarrow Ca_2PbO_4 + Cl_2 + 2CO_2 \quad (5)$$

It is noted that the phase of CaO is not observed in partially reacted lime particles (pure or doped). This is due to the fact that the equilibrium of the reversible reaction $CaO + CO_2 \rightleftarrows CaCO_3$ favors the formation of $CaCO_3$ at 700 °C under 15% of carbon dioxide. Therefore, CaO is completely converted to $CaCO_3$ before all CaO reacts with $PbCl_2$.

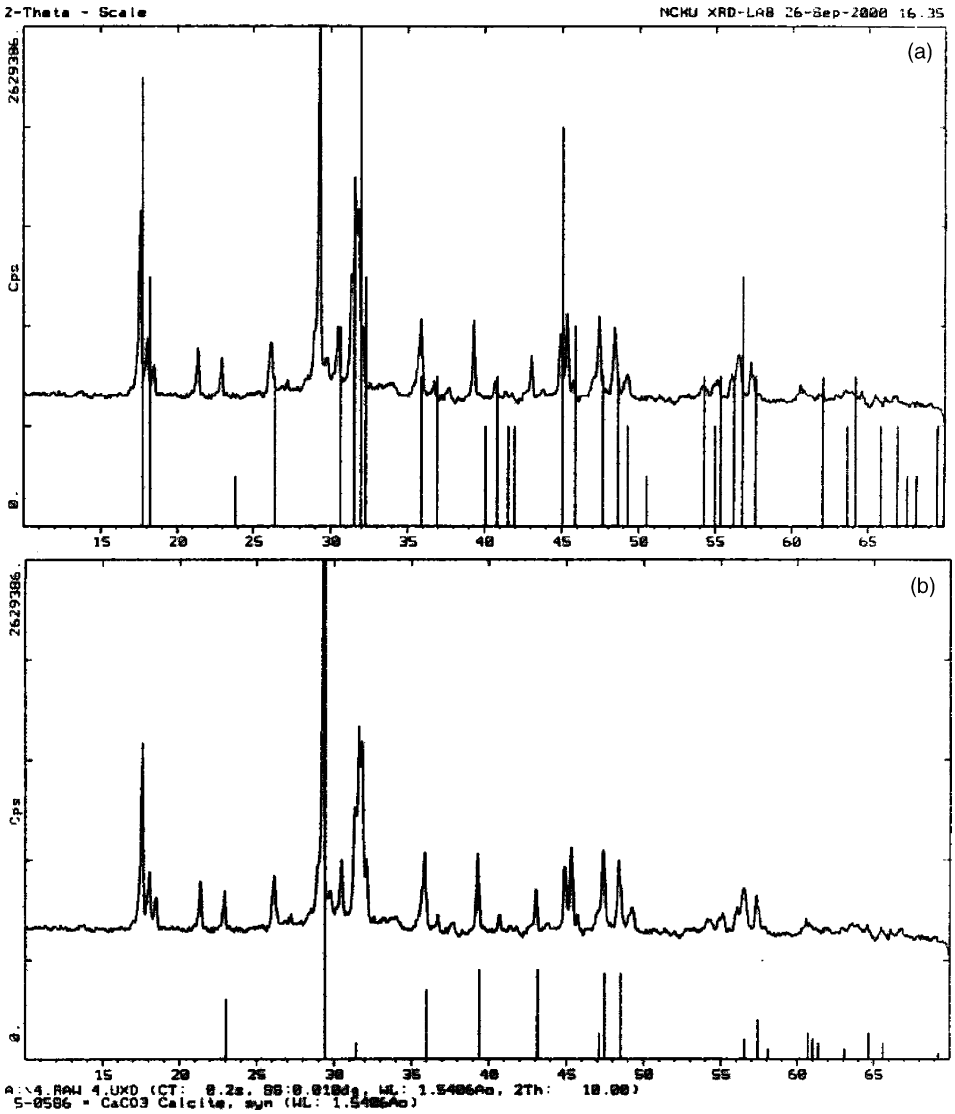

Fig. 13. (a) X-ray diffraction pattern of partially converted lime particles (pure or impregnated with 2 mol% $CaCl_2$) and the standard XRD pattern of Ca_2PbO_4; (b) X-ray diffraction pattern of partially converted lime particles (pure or impregnated with 2 mol% $CaCl_2$) and the standard XRD pattern of $CaCO_3$.

The above mentioned excellent performance of the doped CaO strongly stimulated us to understand further the reason for the morphological changes of doped lime particles during lead sorption.

Fig. 4 is a typical SEM image of the surfaces of partially converted pure lime particles. After lead sorption, a porous aspect of pure lime particles has changed to the rugged

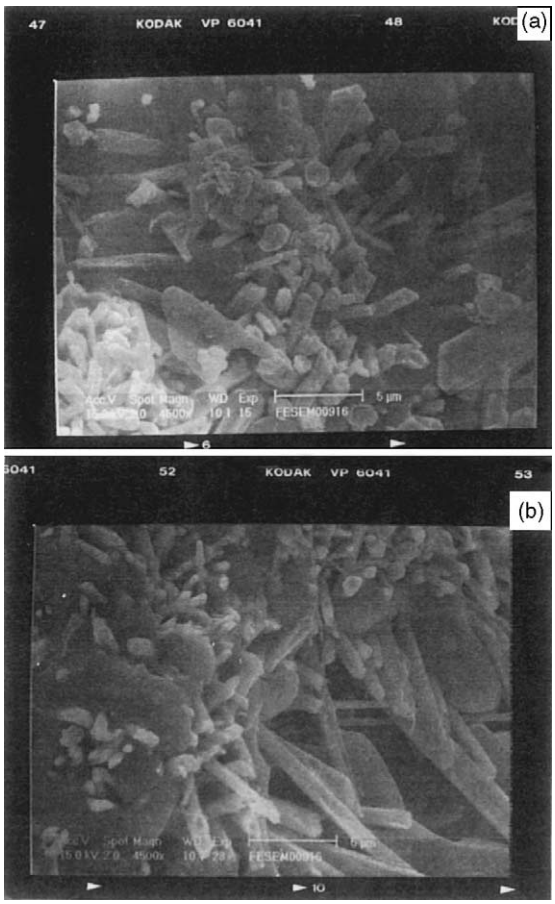

Fig. 14. Morphological change in the surface of the doped CaO. (a and b) Magnification 4500×, sorption conducted at 700 °C for 40 min, concentration of $PbCl_2$: 8.1×10^{-5} g mol/l.

morphology, indicating the formation of the final products on the lime surfaces and a complete disappearance of the cracks. As shown in Fig. 14(a) and (b), a different morphological aspect is observed for the doped CaO after lead sorption. It seems that the promoting effect of the additive is to bring about the formation of the products with a more favorable and less compact texture. This less impervious texture seemingly plays an interesting role of paths through which the interior of lime particles is more easily accessible to $PbCl_2$, leading to much higher capacity of the doped CaO for lead removal.

3.3. Adsorption of multiple compounds through the multi-functional sorbent

In most practical applications of sorbents, a number of contaminants are present in the flue gases and therefore influence the sorption processes. In most cases, the interactions

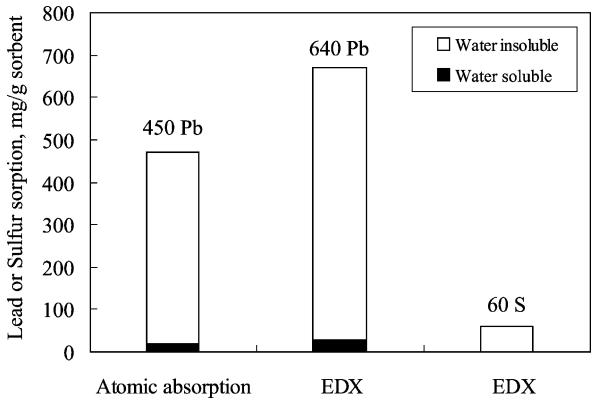

Fig. 15. Lead or sulfur uptake by CaO (impregnated with $CaCl_2$) in 20 min, $T = 700\,^{\circ}C$, concentration of $PbCl_2$: 1.63×10^{-4} g mol/l, concentration of SO_2: 5.7×10^{-5} g mol/l.

of various compounds are complex and little understood. In fact, the simultaneous sorption has received very little attention in the sorbent studies. The present study is the first phase of the development of a multi-functional sorbent that is underway in our laboratory.

The presence of SO_2 in the gas phase along with $PbCl_2$ can result in various interactions. Possible interplay could include a gas phase reaction between SO_2 and $PbCl_2$, a gas–solid reaction between $CaSO_4$ and $PbCl_2$, leading to the formation of complexes; or independent sorbent/species interactions with the formation of both $CaSO_4$ and Ca_2PbO_4.

To determine the effect of SO_2 on lead capture, the sorption experiments were carried out with 5.7×10^{-5} g mol/l of SO_2 and 1.63×10^{-4} g mol/l of $PbCl_2$ in the gas phase. The doped CaO is exposed to the simulated flue gas for a duration of 20 min. The results, as shown in Fig. 15, indicate that the doped CaO can capture both $PbCl_2$ and SO_2 from the simulated flue gases. They also show that the lead adsorption capacity of the doped CaO is not affected even though the flue gas contains 5.7×10^{-5} g mol/l of SO_2. The X-ray diffraction spectra obtained for the doped CaO after the simultaneous sorption of lead and SO_2 are shown in Fig. 16. They reveal the formation of $CaCO_3$, $CaSO_4$, and Ca_2PbO_4 during simultaneous sorption process. The formation mechanism of these compounds has been discussed previously.

To further understand the reason for effectiveness of the doped CaO in lead removal in the presence of SO_2, the SEM images of the surfaces of the pure and doped CaO particles were obtained and shown in Figs. 17 and 18. The results for the pure particles in Fig. 17 show that after sorption, the original porous aspect of the pure CaO particles has changed to the rugged morphology, resulting in a complete disappearance of the cracks. For the doped CaO particles, the results shown in Fig. 18 demonstrate that, in the simultaneous sorption of both SO_2 and $PbCl_2$, the newly formed crystals on the surfaces of the reacted lime particles are flower-shaped. The formation of $CaCO_3$, $CaSO_4$, and Ca_2PbO_4 is supposed to cause the pore closure because the molar volumes of $CaCO_3$, $CaSO_4$, and Ca_2PbO_4 are larger than that

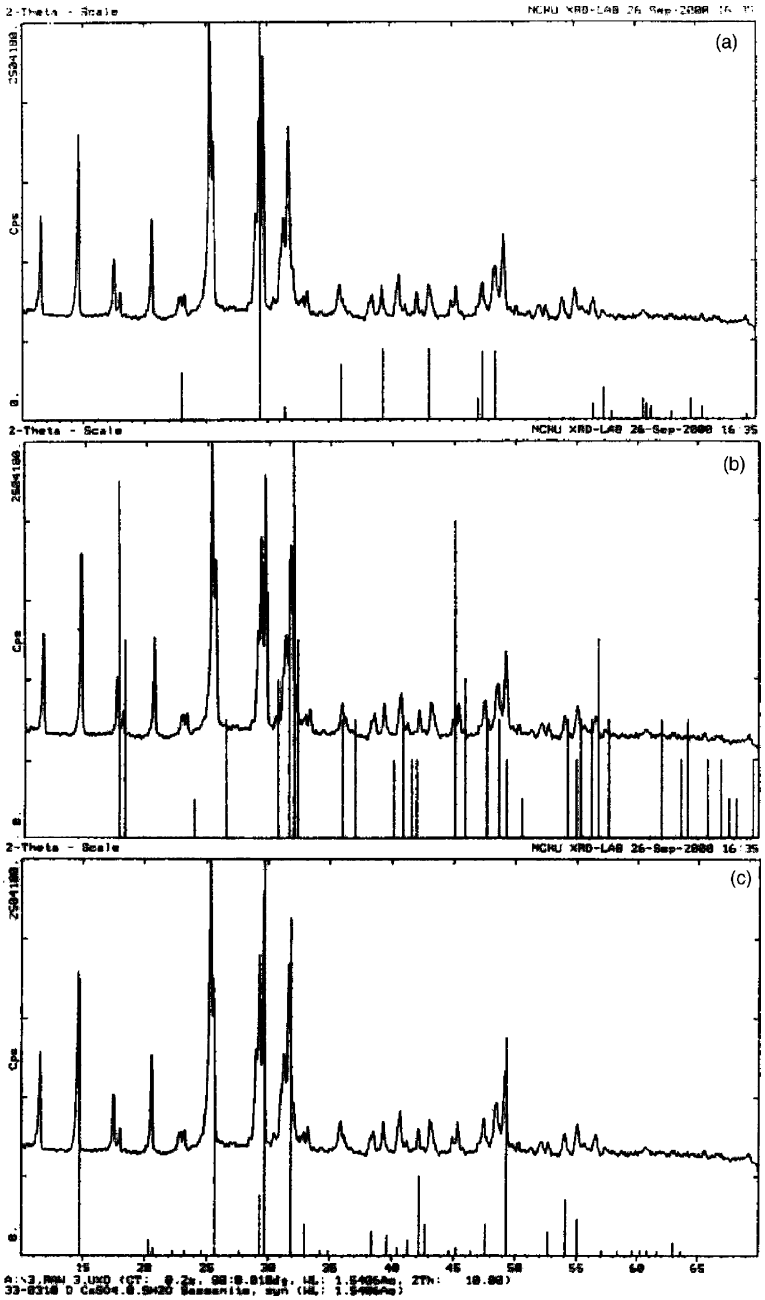

Fig. 16. (a) X-ray diffraction pattern of partially converted lime (impregnated with 2 mol% $CaCl_2$) and the standard XRD pattern of $CaCO_3$, (b) X-ray diffraction pattern of partially converted lime particles (impregnated with 2 mol% $CaCl_2$) and the standard XRD pattern of Ca_2PbO_4, (c) X-ray diffraction pattern of partially converted lime (impregnated with 2 mol% $CaCl_2$) and the standard XRD pattern of $CaSO_4$ $0.5H_2O$.

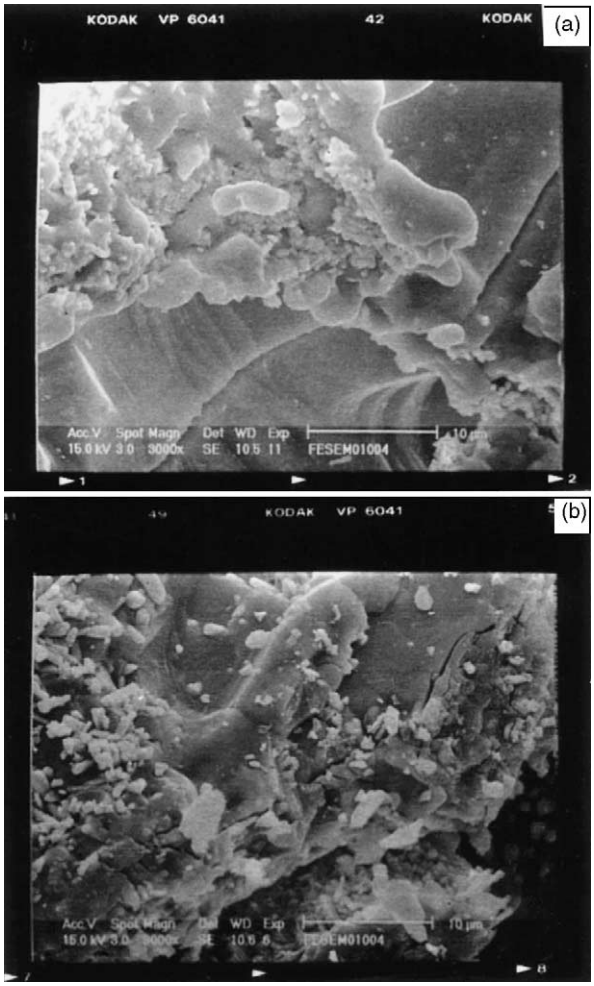

Fig. 17. Morphological change in the surface of CaO: (a) after 20 min of the combined adsorption of sulfur and lead, magnification 3000×; (b) after 20 min of the combined adsorption of sulfur and lead, magnification 3000×.

of calcium oxide. Instead, the numerous voids on the surfaces were formed. This suggests that the recrystallization of the products takes the form of a more open polycrystalline structure in the presence of $CaCl_2$. This interesting polycrystallization pattern could be the result of a decrease of the rate of nucleation of $CaSO_4$ and Ca_2PbO_4 crystallites, or of a more active crystal growth, or of the adoption, by the growing crystals, of a habit different from the habit that they have when pure. The porous structure newly formed after exposure of the doped CaO to both SO_2 and $PbCl_2$ greatly enhances the availability of the interior of the lime particles, leading to no loss of activity of the doped CaO even though in the presence of SO_2 in the simulated flue gases.

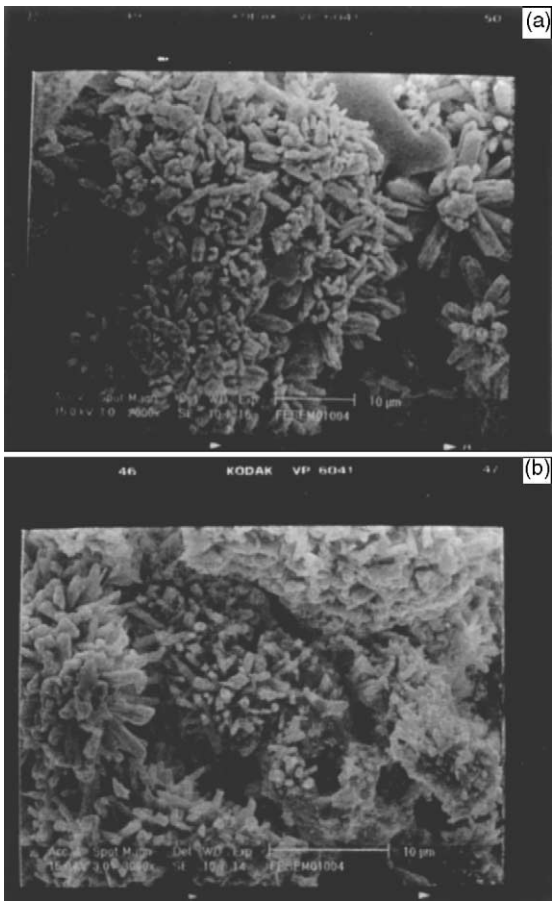

Fig. 18. Morphological change in the surface of CaO impregnated with $CaCl_2$: (a) after 20 min of the combined adsorption of sulfur and lead, magnification 2000×; (b) after 20 min of the combined adsorption of sulfur and lead, magnification 3000×.

4. Conclusions

The new multi-functional sorbent in this study is effective in the simultaneous removal of sulfur and lead compounds from the simulated flue gases at 700 °C. The individual $PbCl_2$ capture occurs by a chemical reaction between $CaO/CaCO_3$ and $PbCl_2$, with Ca_2PbO_4 formed as the final product. The combined removal of SO_2 and $PbCl_2$ takes place by the chemical reactions between the multi-functional sorbent and contaminants in the simulated flue gas, forming $CaSO_4$ and Ca_2PbO_4. Consequently, sulfur and lead compounds are transferred from vapor to a solid phase and therefore can be controlled more easily in the baghouses or electrostatic precipitators of the incineration systems. The overall sorption process is a complex combination of adsorption, condensation, diffusion and chemical

reactions. The product layer is a porous molten structure in the case of individual SO_2 sorption and a flower-shaped polycrystalline structure in the case of the combined adsorption of lead and sulfur compounds. The tailored sorbent is effective in the simultaneous removal of the tested contaminants. The present study is the first phase of a comprehensive investigation on the interactions among sulfur, lead compounds and the lime particles. The intrinsic kinetics of the adsorption/reaction under different operating conditions is still under investigation in our laboratory.

Acknowledgements

The authors are grateful for the financial support of this work by the National Science Council of the Republic of China under grant NSC 89-2214-E-274-001.

References

[1] C.A. Cole, S.A. Kressin, in: Proceedings of the 16th Mid-Atlantic Industrial Waste Conference on Toxic and Hazardous Wastes, Technomic Publishing Co., 1984, pp. 215–216.
[2] R.G. Barton, P.M. Maly, in: Proceedings of the 1998 Conference on Natural Waste, 1988, pp. 378–385.
[3] A.P. Mathews, in: R. Abbou (Ed.), Hazardous Waste: Detection, Control, Treatment, Elsevier, Amsterdam, 1988, p. 593.
[4] M. Uberoi, F. Shadman, AIChE J. 36 (1990) 307.
[5] A.E. Holland, E.R. Segnit, T.J. Gelb, J. Eng. Power 102 (1980) 397.
[6] E.N. Cantwell, E.S. Jacobs, Control of particulate lead emissions from automobiles, in: Proceedings at Natural SAE Meeting, Paper No. 720672, Detroit, MI, 1972.
[7] M. Uberoi, F. Shadman, Environ. Sci. Technol. 25 (1991) 1295.
[8] M.V. Scotto, M. Uberoi, Fuel Proc. Technol. 39 (1994) 357.
[9] W.P. Linak, Combust. Sci. Technol. 101 (1994) 7.
[10] T.C. Ho, C. Chen, J.R. Hopper, Combust. Sci. Technol. 85 (1992) 101.
[11] R. Agnihotri, S. Chauk, S. Mahuli, L.S. Fan, Environ. Sci. Technol. 32 (1998) 1841.
[12] B.C. Wu, F. Shadman, Environ. Sci. Technol. 29 (1995) 1660.
[13] A. Ghosh-Dastidar, S.K. Mahuli, Ind. Eng. Chem. Res. 35 (2) (1990) 598.
[14] C.R. Milne, G.D. Silcox, D.W. Pershing, D.A. Kirchgessner, Ind. Eng. Chem. Res. 29 (11) (1990) 2201.
[15] J.C. Haartz, M.E. Peter, Anal. Chem. 51 (13) (1979) 2293.
[16] G. Van Houte, L. Rodrique, M. Genet, Environ. Sci. Technol. 15 (1981) 327.
[17] L.E. Derlyukova, Zh. Neorg. Khim. 18 (1973) 2341.